

Positive–Unlabeled Reinforcement Learning Distillation for On-Premise Small Models

Zhiqiang Kou ^{*1,2} Junyang Chen ^{*2} Xin-Qiang Cai ³ Xiaobo Xia ⁴ Ming-Kun Xie ³ Dong-Dong Wu ³
 Biao Liu ² Yuheng Jia ² Xin Geng ² Masashi Sugiyama ^{3,5} Tat-Seng Chua ⁴

Abstract

Due to constraints on privacy, cost, and latency, on-premise deployment of small models is increasingly common. However, most practical pipelines stop at supervised fine-tuning (SFT) and fail to reach the reinforcement-learning (RL) alignment stage. The main reason is that RL alignment typically requires either expensive human preference annotation or heavy reliance on high-quality reward models with large-scale API usage and ongoing engineering maintenance, both of which are ill-suited to on-premise settings. To bridge this gap, in this paper, we propose a positive–unlabeled (PU) RL distillation method for on-premise small-model deployment. Without human-labeled preferences or a reward model, our method distills the teacher’s preference-optimization capability from black-box generations into a locally trainable student. For each prompt, we query the teacher once to obtain an anchor response, locally sample multiple student candidates, and perform anchor-conditioned self-ranking to induce pairwise or list-wise preferences, enabling a fully local training loop via direct preference optimization or group relative policy optimization. Theoretical analysis justifies that the induced preference signal by our method is order-consistent and concentrates on near-optimal candidates, supporting its stability for preference optimization. Experiments demonstrate that our method achieves consistently strong performance under a low-cost setting.

1. Introduction

Reinforcement learning (RL) has become a key mechanism for aligning large generative models, as preference-based

¹Hong Kong Polytechnic University ²Southeast University
³RIKEN AIP ⁴National University of Singapore ⁵University of Tokyo. Correspondence to: Xiaobo Xia <xbx@nus.edu.sg>.

Preprint. January 29, 2026.

paradigms such as reinforcement learning from human feedback (RLHF) (Ouyang et al., 2022), direct preference optimization (DPO) (Rafailov et al., 2023), and group relative policy optimization (GRPO) (Liu et al., 2024; Guo et al., 2025) can improve behaviors beyond static demonstrations. However, many real-world deployments prefer on-premise small expert models due to privacy, cost, latency, and compliance constraints (Touvron et al., 2023; Gunasekar et al., 2023). In principle, such models follow the standard recipe of downstream supervised fine-tuning (SFT) adaptation followed by preference-based RL alignment (Zhou et al., 2023). Unfortunately, in practice, the RL stage is often infeasible on-premise: sustainable human preference labeling is costly, training and maintaining a reliable reward model is non-trivial, and high-quality alignment data are generally unavailable (Casper et al., 2023). While cloud providers may accumulate large-scale instruction and preference corpora, these data cannot be shared due to proprietary and regulatory constraints (Li et al., 2023a). As a result, on-premise expert models typically stop at SFT and lack RL-driven self-improvement capability.

As illustrated in Figure 1, it is natural to leverage a stronger foundation model to guide an on-premise small model. Nevertheless, existing solutions largely fall into two paradigms, both with clear limitations. The first paradigm is *imitation-based distillation* (Li et al., 2022; Lin et al., 2020), shown in Figure 1(a), where the teacher provides responses (or logits) and the student is trained via SFT to mimic these demonstrations. While effective at transferring task competence, this paradigm relies on static examples and fails to impart preference-optimization–driven self-improvement. The second paradigm is *teacher-as-judge* RL (Yuan et al., 2024a; Lee et al., 2023), as shown in Figure 1(b). For each prompt, the student samples multiple candidate responses, and the teacher or an auxiliary reward model scores or ranks all candidates to produce scalar rewards for RL. Although this paradigm reduces explicit human annotation, it is cost-prohibitive and throughput-limited in on-premise settings. In particular, with N prompts and K candidates per prompt, the judge must evaluate approximately NK responses, resulting in $\mathcal{O}(NK)$ teacher calls and largely increased token consumption and latency variance.

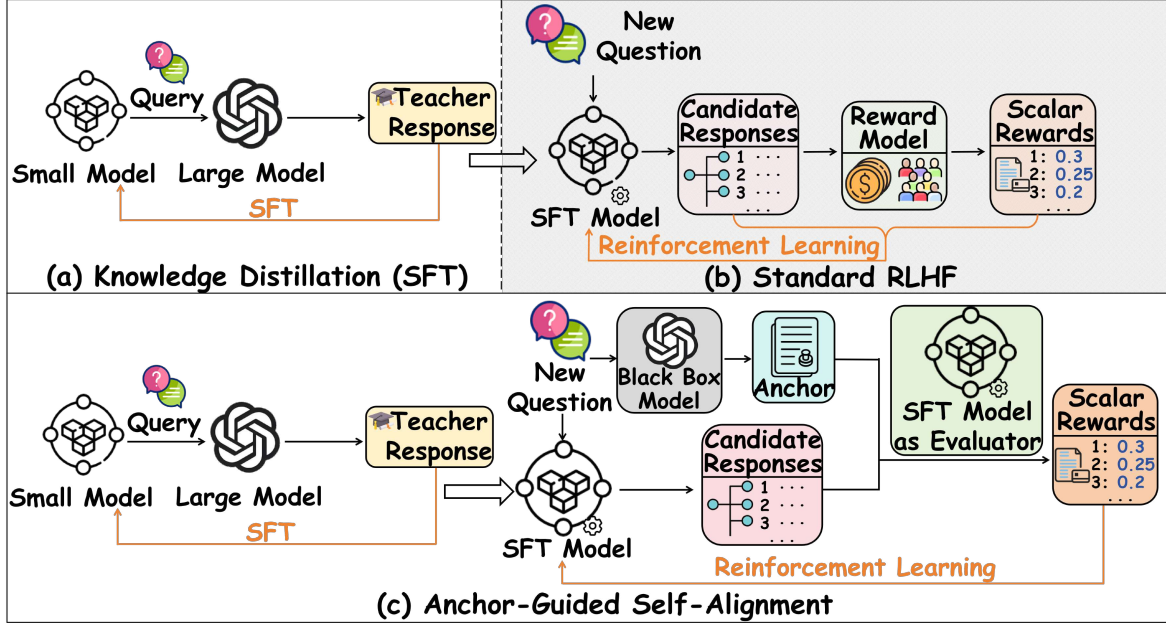


Figure 1. Comparison among SFT, RLHF, and anchor-guided self-alignment (ours). For on-premise small-model deployment, training pipelines typically stop at the first-stage SFT: the small model imitates black-box teacher responses but fails to acquire preference-optimization-driven self-improvement. The second-stage RL alignment is hard to realize locally because it relies on large-scale human annotations or extensive reward-model calls. We propose a low-cost on-premise alignment strategy: for each query, we call the black-box teacher once to obtain an anchor and use anchor-guided local sampling and self-evaluation to generate scalar signals, enabling a practical SFT-to-RL loop under strict cost and deployment constraints.

Based on the above observations, we raise a more fundamental question: can we distill the *preference-optimization* capability of RL from a black-box large model into an on-premise small model *without* human preference labels or a reward model? We formalize this as *Reinforcement Learning Capability Distillation* (RLCD), where the teacher model is only accessible via black-box generation while the student is white-box and can be locally sampled and updated. The goal is to enable *low-cost* and sustainable preference-based alignment under strict on-premise constraints.

To achieve RLCD, we adopt a *PU-based anchor preference induction* mechanism (Kirylo et al., 2017; Niu et al., 2016; Garg et al., 2021). For each prompt x , we query the teacher once to obtain a high-quality response y^+ as an implicit *positive anchor*, and locally sample a set of student candidates $\{y_k\}_{k=1}^K$, treated as *unlabeled* data that may include both latent positives and inferior negatives. Conditioned on the anchor, the student performs *self-ranking* over its own candidates to induce relative preference relations, which are directly used by preference-optimization objectives such as DPO and GRPO. This forms a fully local “sampling–comparison–update” RL loop. Crucially, the anchor is *not* a judge: the teacher is used only to produce the anchor and never scores or ranks student outputs. All preference signals are induced locally, reducing teacher dependence from $\mathcal{O}(NK)$ candidate evaluations to $\mathcal{O}(N)$ one-anchor-per-prompt queries and eliminating the need for

a reward model, thereby meeting on-premise constraints on cost, throughput, and compliance.

We provide both theoretical and empirical support for our method. On the theoretical side, we show that the anchor-induced PU preference signal yields an order-consistent and well-concentrated listwise supervision, which justifies its use for stable preference optimization. Empirically, we evaluate our method on representative on-premise expert tasks across unimodal and multimodal settings, including writing, mathematical reasoning, and image captioning. Under the same or even lower teacher-query budget, our method consistently outperforms SFT, output distillation, and teacher-as-judge baselines. Together, these results demonstrate that, using only black-box teacher generations and without human preferences or a reward model, it is possible to distill the RL capability into small on-premise models, enabling a practical local alignment pipeline from SFT to RL. Our contributions are summarized as follows:

- We formulate RLCD, which studies how to distill preference-optimization–driven RL capability from a black-box large model into an on-premise small model without human preferences or reward models.
- We propose two PU-based anchor preference induction methods that enable fully local alignment, which reduces teacher dependence effectively without requiring

reward-model training.

- Theoretical guarantees are provided to show that the induced listwise preference supervision by our method can be order-consistent and concentrates on near-optimal candidates.
- Empirical results are offered to demonstrate consistent improvements over strong baselines across unimodal and multimodal on-premise tasks under the same or lower teacher-query budget.

2. Related Work

In this section, we review recent literature related to this work, including preference-based alignment, knowledge distillation (KD) for on-premise language models, and self-rewarded reinforcement learning.

2.1. Preference-Based Alignment

Reinforcement learning from human feedback (RLHF) has emerged as a dominant paradigm for aligning large language models with human intent and preferences (Ouyang et al., 2022). A canonical RLHF pipeline typically combines supervised fine-tuning (SFT) on curated instruction-response data with preference optimization based on human-annotated comparisons, often implemented through a learned reward model and RL algorithms such as proximal policy optimization (PPO) (Schulman et al., 2017). Subsequent studies have proposed more stable and simplified alternatives that directly optimize preference objectives (Rafailov et al., 2023), including reward-model-free formulations that bypass explicit reinforcement learning while still relying on preference pairs (Ethayarajh et al., 2024). Despite their effectiveness, most RLHF-style methods implicitly rely on the availability of at least one of the following: (i) curated instruction–answer datasets, (ii) human-annotated preference comparisons, or (iii) a reliable reward model. These assumptions are frequently violated in on-premise deployment settings, where privacy constraints and domain specificity restrict data sharing, and where constructing a high-quality reward model is costly, impractical, or even infeasible (Yuan et al., 2024b).

2.2. KD for On-Premise Language Models

Knowledge distillation (KD) (Gou et al., 2021; Park et al., 2019a; Wang & Yoon, 2021) transfers capabilities from a strong teacher model to a weaker student by using the teacher’s outputs as supervision, and has been widely adopted to compress large models into deployable ones (Hinton et al., 2015; Kim & Rush, 2016; Zhang et al., 2019; Phuong & Lampert, 2019; Yang et al., 2023; Park et al., 2019b; Xiang et al., 2025; Yu et al., 2025; Wei et al., 2025).

In the context of large language models, a prevalent practice is instruction distillation, where a powerful teacher is queried to generate high-quality responses for a pool of prompts, and the student is subsequently trained via SFT to imitate these teacher-generated outputs (Sun et al., 2023; Wang et al., 2023; Hsieh et al., 2023; Li et al., 2023b). Such strategies are particularly attractive for on-premise deployment, as they avoid direct exposure of private data and can operate with black-box access to hosted teacher models. However, most prior distillation methods primarily focus on transferring static knowledge or single-shot response quality, by matching the teacher’s outputs on individual prompts (Ouyang et al., 2022). As a result, they largely overlook the distillation of the teacher’s preference-optimization or self-improvement capabilities (Tunstall et al., 2023), which are typically acquired through alignment training.

2.3. Self-Rewarded Reinforcement Learning

A complementary line of research explored how language models can improve generation quality with minimal external supervision, e.g., through self-critique, self-refinement, or iterative bootstrapping (Madaan et al., 2023; Zelikman et al., 2022; Tian et al., 2024; Yin et al., 2025; Shridhar et al., 2024; He et al., 2025). Related works further attempted to replace human feedback with model-generated signals, including self-rewarding (Yuan et al., 2024a) and self-judging schemes (Lee et al., 2023) in which a model evaluates its own candidates and uses the resulting feedback for policy improvement (Yuan et al., 2024b; Bai et al., 2022; Zheng et al., 2023; Thawakar et al., 2025; Zhou et al., 2024). Despite their promise, purely self-driven signals are often unstable and prone to drift (Shumailov et al., 2023), whereas teacher-as-judge pipelines can be computationally expensive because they require scoring each candidate individually. In contrast, our method adopts a single teacher anchor as a high-confidence positive exemplar and elicits a groupwise soft preference distribution via in-context self-judging. This design enables iterative preference optimization using only local computation, without relying on explicit preference pairs or a learned reward model.

3. Method

In this section, we first offer some background knowledge and then introduce our method step by step. Finally, theoretical results are provided to justify our claims.

3.1. Preliminaries

Common on-premise alignment pipeline. In an ideal on-premise deployment, one starts from a general base model $p_{\text{base}}(\cdot|x)$ and performs supervised fine-tuning (SFT) on local SFT pairs $\mathcal{D}_{\text{sft}} = \{(x, y)\}$ to obtain an instruction-following model $p_{\text{sft}}(\cdot|x)$. Afterward, preference-based re-

inforcement learning (*e.g.*, RLHF or DPO) is applied using human-labeled preference tuples $\mathcal{D}_{\text{pref}} = \{(x, y^+, y^-)\}$ to produce the final aligned model $p_{\text{rl}}(\cdot|x)$. Here, y^+ and y^- denote the preferred and non-preferred responses for the same prompt x , respectively.

Overall objective. Given an unlabeled query pool \mathcal{D}_x and black-box access to a teacher model T , our goal is to learn an on-premise student model $p_{\text{rl}}(\cdot|x)$ that acquires reinforcement-learning capability under a strictly limited teacher-query budget. Specifically, we aim to: (i) query the teacher at most once per prompt to obtain an anchor response $a = T(x)$; (ii) perform all subsequent exploration, comparison, and parameter updates locally using student-sampled candidates $U(x) = \{y_k\}_{k=1}^K$; and (iii) optimize the student via preference-based updates, without relying on human preference pairs or an explicit reward model. Below, we introduce the proposed method step by step. The algorithmic flow is provided in Algorithm 1.

3.2. Stage I: Teacher-Guided SFT

Although our ultimate goal is to distill reinforcement-learning capability, we first warm-start the on-premise student to ensure basic instruction following and a reasonable generation prior. This setting follows the standard cold-start practice adopted in prior work, *e.g.*, (Guo et al., 2025). Specifically, given an unlabeled query pool \mathcal{D}_x , we query the black-box teacher model T once per prompt to obtain a response $y = T(x)$ and construct an SFT dataset $\mathcal{D}_{\text{sft}} = \{(x, y)|x \in \mathcal{D}_x\}$. We then fine-tune the on-premise student, starting from a base model $p_{\text{base}}(\cdot|x)$ by minimizing the standard maximum-likelihood objective:

$$\min_{\theta} \mathbb{E}_{(x,y) \sim \mathcal{D}_{\text{sft}}} [-\log p_{\theta}(y|x)]. \quad (1)$$

This stage corresponds to conventional SFT using teacher-generated responses as training targets, without introducing any preference signals, ranking supervision, or reinforcement-learning updates. The resulting model, denoted as $p_{\text{sft}}(\cdot|x)$, serves as a well-initialized starting point for Stage II, where the student is further improved through preference-based optimization rather than direct imitation.

3.3. Stage II: Reinforcement Learning Capability Distillation (RLCD)

Anchor-conditioned PU self-evaluation. Stage II adopts a positive-unlabeled (PU) formulation (Kiryo et al., 2017; Niu et al., 2016) tailored to low-cost on-premise alignment. For each query x , we associate each response with a latent quality indicator $z \in \{0, 1\}$, where $z = 1$ denotes a preferred response and $z = 0$ otherwise. As there are no ground-truth answers, human preference pairs, or reward model are available, the student’s sampled responses are treated as unlabeled. We therefore query the black-box teacher

once to obtain an anchor response a , which serves as a high-confidence *positive seed* as $T(x) = a$. The student then locally samples K candidates $\{y_k\}_{k=1}^K$ with $y_k \sim p_{\theta}(\cdot|x)$, forming an unlabeled set $U(x) = \{y_k\}_{k=1}^K$ that contain good and bad responses and may contain *latent positives*.

To transform the single positive seed into a dense training signal over $U(x)$, we adopt *PU in-context inference*. The anchor a serves as an in-context reference for both correctness and style, enabling the student to *self-evaluate* its sampled candidates without external supervision. Specifically, for each $y_k \in U(x)$, the student produces a scalar utility score $s_k = g_{\theta}(x, a, y_k)$, where g_{θ} is a scoring function induced by the SFT-initialized student model $p_{\text{sft}}(\cdot|x)$, and only the relative magnitudes of $\{s_k\}_{k=1}^K$ will be used later. The resulting scores induce a listwise ranking over $U(x)$ purely from local computation, without requiring an external judge or an explicit reward model.

A naive reranking that treats low-score candidates as negatives is unreliable under the PU setting, as $U(x)$ may contain alternative correct responses. We therefore calibrate scores using the positive seed itself. Let $s^* = g_{\theta}(x, a, a)$ and define the anchor-referenced margin $r_k := s_k - s^*$. We map this margin to a soft positivity confidence $u_k = \sigma(\gamma r_k)$, where $\gamma > 0$ is a softness parameter and σ denotes the Sigmoid activation function. A PU-aware label distribution over the group is then constructed as follows:

$$w_k \propto u_k \exp(r_k/\tau), D_x(k) = \frac{w_k}{\sum_{j=1}^K w_j} \in \Delta^{K-1}, \quad (2)$$

where τ is a temperature parameter and Δ denotes the probability simplex. This formulation allows a single teacher-provided anchor to induce a dense soft preference distribution D_x over $U(x)$ via PU-aware in-context self-evaluation. Given the induced soft preference distribution $D_x \in \Delta^{K-1}$ over $U(x)$, we instantiate RLCD via label distribution learning (LDL) and propose *LDL-GRPO*, which aligns the group-level policy allocation on $U(x)$ with D_x through distribution matching. We next introduce the *LDL-GRPO* formulation.

LDL-GRPO. Given the induced soft preference label distribution $D_x \in \Delta^{K-1}$ over the candidate set $\{y_k\}_{k=1}^K$, our goal is to update the on-premise student such that, within this group, it allocates probability mass in accordance with D_x . This realizes preference optimization *without* an external reward model: the training signal is the distributional supervision D_x derived from anchor-conditioned in-context self-evaluation. Since D_x is defined on candidate indices, we first map the student policy to the same space by normalizing its *unnormalized sequence likelihoods* over the sampled group:

$$q_{\theta}(y_k|x) := \frac{\exp(\log p_{\theta}(y_k|x))}{\sum_{j=1}^K \exp(\log p_{\theta}(y_j|x))} = \frac{p_{\theta}(y_k|x)}{\sum_{j=1}^K p_{\theta}(y_j|x)}. \quad (3)$$

In practice, q_θ is computed via sequence log-likelihoods for numerical stability. We then minimize the divergence between the target label distribution D_x and the candidate-normalized policy distribution $q_\theta(\cdot|x)$, while constraining the updated policy to stay close to a fixed reference model p_{sft} . The resulting *LDL-GRPO* objective is

$$\min_{\theta} \mathbb{E}_x [\text{KL}(D_x \parallel q_\theta(\cdot|x))] + \beta \mathbb{E}_x [\text{KL}(p_\theta(\cdot|x) \parallel p_{\text{sft}}(\cdot|x))]. \quad (4)$$

where $\beta > 0$ is a hyperparameter to balance the two loss terms. Since $\text{KL}(D_x \parallel q_\theta) = \sum_k D_x(k) \log D_x(k) - \sum_k D_x(k) \log q_\theta(y_k|x)$, the first term in Eq. (4) is equivalent, up to an additive constant independent of θ , to minimizing the cross entropy $\sum_k D_x(k) (-\log q_\theta(y_k|x))$. That is,

$$\min_{\theta} \mathbb{E}_x \left[- \sum_{k=1}^K D_x(k) \log p_\theta(y_k|x) + \log \sum_{j=1}^K p_\theta(y_j|x) \right] + \beta \mathbb{E}_x [\text{KL}(p_\theta(\cdot|x) \parallel p_{\text{sft}}(\cdot|x))]. \quad (5)$$

This form makes clear that *LDL-GRPO* increases the likelihood of candidates weighted by D_x , while accounting for the group-wise normalization. Overall, *LDL-GRPO* implements a fully local loop: sample a candidate group \rightarrow induce a PU-aware soft label distribution via anchor-conditioned self-evaluation \rightarrow update the policy by matching its group-wise probability allocation to D_x , requiring neither human preference pairs nor a reward model.

3.4. Theoretical Justification

We provide the following two theoretical results to support our method. The first theorem ensures that D_x is a strictly order-preserving listwise preference signal. The second theorem shows that D_x concentrates on near-best candidates within the sampled set, with a gap controlled by two factors. These properties justify using D_x as a label-distribution target for LDL-GRPO update, turning anchor-seeded PU preference induction into stable group-level supervision without explicit rewards or external judging.

Theorem 3.1 (Order consistency). *For any $i, j \in \{1, \dots, K\}$, $r_i > r_j$ implies $D_x(i) > D_x(j)$.*

Proof sketch. Let $f(r) = \log \sigma(\gamma r) + r/\tau$ so that $D_x(k) \propto \exp(f(r_k))$. Since $f'(r) = \gamma(1 - \sigma(\gamma r)) + 1/\tau > 0$ for all r , f is strictly increasing, which preserves the ordering induced by $\{r_k\}$. Detailed proof is provided in Appendix B.1. \square

Remark 1. Theorem 3.1 guarantees that the PU gating $\sigma(\gamma r)$ does not distort rankings: for any fixed $\gamma > 0$ and $\tau > 0$, D_x induces exactly the same ordering as the calibrated margins $\{r_k\}_{k=1}^K$. In particular, replacing hard pair

Algorithm 1 Pseudo-Code for *LDL-GRPO*

1: **Input:** unlabeled prompt pool \mathcal{D}_x ; black-box teacher T ; student policy p_θ (initialized from p_{sft}); frozen reference p_{sft} ; #candidates K ; temperatures γ, τ ; KL weight β .
 2: **Output:** aligned student p_θ .
 3: **while** not converged **do**
 4: Sample mini-batch $\{\mathbf{x}_i\}_{i=1}^B \sim \mathcal{D}_x$.
 5: **for** $i = 1$ **to** B **do**
 6: *One-shot teacher response*: $\mathbf{a}_i \leftarrow T(\mathbf{x}_i)$.
 7: *Local sampling*: draw K candidates $\mathbf{y}_{i,k} \sim p_\theta(\cdot|\mathbf{x}_i)$.
 8: $s_i^* \leftarrow g_\theta(\mathbf{x}_i, \mathbf{a}_i, \mathbf{a}_i)$.
 9: **for** $k = 1$ **to** K **do**
 10: $r_{i,k} \leftarrow g_\theta(\mathbf{x}_i, \mathbf{a}_i, \mathbf{y}_{i,k}) - s_i^*$.
 11: $\tilde{D}_i(k) \leftarrow \sigma(\gamma r_{i,k}) \exp(r_{i,k}/\tau)$.
 12: $\tilde{q}_i(k) \leftarrow p_\theta(\mathbf{y}_{i,k}|\mathbf{x}_i)$.
 13: **end for**
 14: $D_i \leftarrow \text{Normalize}(\tilde{D}_i)$.
 15: $q_i \leftarrow \text{Normalize}(\tilde{q}_i)$.
 16: **end for**
 17: Update θ by minimizing $\frac{1}{B} \sum_{i=1}^B \text{KL}(D_i \parallel q_i) + \beta \frac{1}{B} \sum_{i=1}^B \text{KL}(p_\theta(\cdot|\mathbf{x}_i) \parallel p_{\text{sft}}(\cdot|\mathbf{x}_i))$ (cf., Eq. (4)).
 18: **end while**

construction by listwise supervision with D_x is consistent with the student’s anchor-referenced comparisons.

Theorem 3.2 (Near-optimality on the sampled set). *Let $r_{\max} = \max_{1 \leq k \leq K} r_k$. Then*

$$r_{\max} - \mathbb{E}_{k \sim D_x}[r_k] \leq \tau \log K. \quad (6)$$

Proof sketch. Define the softmax distribution $\bar{D}(k) = \exp(r_k/\tau) / \sum_{j=1}^K \exp(r_j/\tau)$. A standard log-sum-exp bound gives $\mathbb{E}_{\bar{D}}[r_k] \geq r_{\max} - \tau \log K$ (Boyd & Vandenberghe, 2004). Moreover,

$$D_x(k) = \frac{\bar{D}(k) \sigma(\gamma r_k)}{\sum_{j=1}^K \bar{D}(j) \sigma(\gamma r_j)},$$

which is obtained by reweighting \bar{D} with the increasing factor $\sigma(\gamma r_k)$, thereby shifting probability mass toward larger margins and ensuring $\mathbb{E}_{D_x}[r_k] \geq \mathbb{E}_{\bar{D}}[r_k]$. Combining the two inequalities yields (6). Detailed proof is provided in Appendix B.2. \square

Remark 2. The bound in (6) is controlled only by the sampling budget K and temperature τ : larger K makes the sampled set more likely to contain strong candidates, while smaller τ tightens concentration around high-margin responses. Importantly, the PU term $\sigma(\gamma r)$ can only improve concentration relative to the pure softmax \bar{D} , since it monotonically upweights larger margins.

4. Experiments

4.1. Setups

Datasets and Models. We evaluate our method in both unimodal and multimodal settings. For the unimodal setting, we consider two representative tasks: creative writing and mathematical reasoning. For creative writing, we employ WritingPrompts (Fan et al., 2018) and report results on two variants, WritingPrompts-CW and WritingPrompts-EU. For mathematical reasoning, we use Competition Math (Hendrycks et al., 2021) and evaluate on CompMath-Count and CompMath-Geometry. For the multimodal setting, we evaluate vision-language understanding on A-OKVQA (Schwenk et al., 2022) under two tasks: A-OKVQA-MC, a multiple-choice visual question answering task, and A-OKVQA-Rationale, which requires generating free-form rationales grounded in the image. Additional task details and evaluation prompts are provided in Appendix C.3.

Backbone Models. As on-premise student backbones, we exploit Qwen2.5-7B-Instruct (Yang et al., 2025b) and LLaMA3-8B-Instruct (Grattafiori et al., 2024) for unimodal tasks, and LLaVA-7B (Liu et al., 2023) and Qwen2.5-VL-7B-Instruct (Bai et al., 2025) for multimodal tasks. Model details and access information are provided in Appendix C.4.

Evaluation Metric. We conduct automatic A/B preference evaluation by comparing each baseline against GPT-4o (the 2024-11-20 version). Specifically, for each query, an external judge selects the better response according to task-specific criteria such as instruction following, correctness, and overall helpfulness. For unimodal text tasks, we adopt Qwen3-235B-A22B-Instruct (Yang et al., 2025a) as the judge model, while for multimodal vision-language tasks, we use Qwen3-VL-235B-A22B-Instruct (Yang et al., 2025a). We report both the raw win rate (Raw) and the length-controlled win rate (LC). The LC metric mitigates potential verbosity bias by enforcing comparable response lengths during evaluation. Ties are counted as half wins for both WR and LC. Additional details on the evaluation protocol and judge models are provided in Appendix C.1.

Baselines. We evaluate the following baselines that are strictly aligned with our stage-wise setting. Note that all methods share the same on-premise student backbone and the same stage-II prompts. They differ only in how supervision signals are constructed and how the student is updated.

- *SFT*. The on-premise model after the first-stage SFT only, with no second-stage preference optimization.
- *SFT*→*SFT*. Starting from the SFT model, we query the black-box teacher on the stage II prompts and continue supervised fine-tuning on the teacher outputs, replacing

RL with additional imitation learning.

- *SinglePair-DPO* (Rafailov et al., 2023). Starting from the SFT model, for each stage II prompt, we obtain one teacher response and one student response, form a single preference pair where the teacher response is preferred, and optimize the student with direct preference optimization.
- *Anchor-GRPO* (Guo et al., 2025). Starting from the SFT model, for each stage II prompt, we query the teacher once to obtain an anchor response, sample multiple student candidates locally, and use the on-premise SFT model as an anchor-conditioned evaluator to score these candidates. The resulting scalar (group-relative) rewards are then used to optimize the student via standard group relative policy optimization.
- *Self-PPO* (Schulman et al., 2017). Starting from the SFT model, we sample a single response per stage II prompt and obtain a scalar self-reward via on-premise self-evaluation. The student is then optimized with proximal policy optimization using this signal, without querying any external teacher or judge during training.
- *AnchorRank-DPO* (Rafailov et al., 2023). Starting from the SFT model, we query the teacher once per stage-II prompt to obtain an anchor, sample multiple student candidates locally, and perform anchor-conditioned self-ranking to induce pairwise preferences. The student is then trained with direct preference optimization on these induced preferences.

Implementation. All methods (except for *SFT*) are implemented within a unified two-stage training pipeline to ensure fair and controlled comparison. We first perform SFT on teacher-generated responses to obtain a warm-started on-premise model that exhibits basic instruction-following ability. This SFT checkpoint is used to initialize all stage II variants. In stage II, all methods are trained on the same prompt set with identical decoding configurations and backbone architectures, and differ only in their optimization objectives and the construction of supervision signals. Specifically, we consider *SFT*→*SFT*, *SinglePair-DPO*, *Anchor-GRPO*, *Self-PPO*, *AnchorRank-DPO*, and *LDL-GRPO*. For anchor-guided methods, the black-box teacher is queried exactly once per prompt to obtain an anchor response, after which all candidate sampling, self-evaluation, and policy updates are performed entirely on-premise. This design ensures that performance differences stem from the learning objectives rather than from unequal teacher access or computational budgets. Detailed implementation settings, training hyperparameters, and evaluation configurations are provided in Appendix C.

Table 1. Main performance comparison of our methods and various baselines. The comparison covers six representative tasks spanning unimodal and multimodal domains. Within each case, the best result is highlighted in bold with a gray background, and the second-best result is underlined.

Method	Qwen2.5-VL-7B				LLaMA3-8B / LLaVA-7B			
	Raw ↑	LC ↑	Raw ↑	LC ↑	Raw ↑	LC ↑	Raw ↑	LC ↑
<i>Writing</i>	<i>Task 1: CFCW</i>				<i>Task 2: PBFG</i>			
<i>SFT</i>	0.538	<u>0.452</u>	0.573	0.513	0.568	0.487	0.482	0.372
<i>SFT</i> → <i>SFT</i>	0.352	<u>0.337</u>	0.372	0.327	0.462	0.387	0.417	0.312
<i>SinglePair-DPO</i>	0.492	0.447	0.477	0.437	0.533	0.432	0.683	0.482
<i>Anchor-GRPO</i>	0.508	<u>0.452</u>	0.548	0.487	0.573	0.513	0.673	0.508
<i>Self-PPO</i>	0.543	<u>0.392</u>	0.658	0.538	0.628	<u>0.518</u>	0.764	0.523
<i>AnchorRank-DPO</i>	<u>0.573</u>	0.417	<u>0.663</u>	<u>0.573</u>	<u>0.643</u>	0.472	<u>0.814</u>	<u>0.608</u>
<i>LDL-GRPO</i> (ours)	0.588	0.553	0.678	0.583	0.683	0.543	0.834	0.623
<i>Math</i>	<i>Task 3: CountProb</i>				<i>Task 4: Geometry</i>			
<i>SFT</i>	0.533	0.487	0.382	0.427	0.613	0.583	0.457	0.437
<i>SFT</i> → <i>SFT</i>	<u>0.558</u>	0.533	0.442	0.417	<u>0.678</u>	<u>0.658</u>	0.608	0.588
<i>SinglePair-DPO</i>	0.462	0.452	0.392	0.382	0.457	0.442	0.397	0.382
<i>Anchor-GRPO</i>	<u>0.558</u>	<u>0.538</u>	0.422	0.397	0.628	0.608	0.452	0.432
<i>Self-PPO</i>	0.518	0.492	0.477	0.462	0.638	0.623	0.583	0.563
<i>AnchorRank-DPO</i>	0.538	0.492	<u>0.492</u>	<u>0.482</u>	0.633	0.598	<u>0.633</u>	0.618
<i>LDL-GRPO</i> (ours)	0.578	0.573	0.508	0.497	0.724	0.709	0.638	0.613
<i>Multimodal</i>	<i>Task 5: A-OKVQA-MC</i>				<i>Task 6: A-OKVQA-RG</i>			
<i>SFT</i>	0.131	0.136	0.131	0.121	0.231	0.226	0.256	0.261
<i>SFT</i> → <i>SFT</i>	0.075	0.065	0.106	0.085	0.075	0.106	0.181	0.171
<i>SinglePair-DPO</i>	0.166	0.171	0.055	0.050	0.106	0.101	0.307	0.276
<i>Anchor-GRPO</i>	0.146	0.156	0.090	0.035	0.151	0.166	0.357	0.327
<i>Self-PPO</i>	0.206	0.216	<u>0.136</u>	<u>0.126</u>	0.241	0.231	0.382	0.362
<i>AnchorRank-DPO</i>	0.216	0.226	0.126	0.121	0.256	0.246	0.412	0.392
<i>LDL-GRPO</i> (ours)	0.236	0.231	0.146	0.141	0.261	0.256	0.432	0.417

4.2. Results and Findings

We provide the comparison between our methods and baselines in Table 1. The results lead to the following findings.

Finding 1. Across all six tasks and backbones, our two anchor-based methods, *AnchorRank-DPO* and *LDL-GRPO*, consistently achieve the top-two performance under both Raw and LC metrics, outperforming all non-anchor baselines. This verifies the effectiveness of distilling preference optimization capability from a single teacher anchor with local exploration.

Finding 2. *LDL-GRPO* outperforms *AnchorRank-DPO* across tasks and model scales, indicating that label-distribution-based group supervision provides more robust and stable preference optimization than multi-pair DPO.

Finding 3. The advantages of anchor-based methods remain clear under LC evaluation, indicating that the improvements are not driven by verbosity. *LDL-GRPO* achieves the highest LC scores on all writing and multimodal tasks.

Finding 4. *SFT*→*SFT* underperforms *SFT*, while all preference-based methods yield clear gains, validating the necessity of a second-stage preference-optimization process.

Finding 5. *AnchorRank-DPO* consistently outperforms *SinglePair-DPO*, showing that inducing preferences from one anchor and multiple local candidates provides richer supervision than single-pair comparisons.

4.3. Ablation Study

We conduct detailed ablation studies across writing, mathematical reasoning, and multimodal tasks, with the comparative results of *SFT*, *Anchor-GRPO*, and our proposed *LDL-GRPO*, as summarized in Table 2. Experimental results indicate that *LDL-GRPO* achieves the highest Raw and LC scores across all benchmarks and backbones, demonstrating stable performance gains over both the *SFT* baseline and *Anchor-GRPO*. Notably, *LDL-GRPO* exhibits superior optimization reliability compared to *Anchor-GRPO*. While *Anchor-GRPO* occasionally exhibits instability under noisy self-evaluation and in some cases underperforms the *SFT* baseline, such as in the A-OKVQA-MC task with the LLaVA-7B backbone, *LDL-GRPO* consistently delivers performance improvements. This behavior suggests that the label distribution learning mechanism effectively mitigates the adverse impact of evaluation noise. Furthermore, these improvements persist under LC evaluation, confirming

Table 2. Ablation study across six representative tasks. We compare *SFT*, *Anchor-GRPO*, and *LDL-GRPO*. Win rates (Raw) and length-controlled win rates (LC) are calculated against GPT-4o. In each case, the best result is bolded with gray shading, and the second-best result is underlined.

Benchmark	Backbone	<i>SFT</i>		<i>Anchor-GRPO</i>		<i>LDL-GRPO</i> (ours)	
		Raw \uparrow	LC \uparrow	Raw \uparrow	LC \uparrow	Raw \uparrow	LC \uparrow
<i>Domain I: Creative Writing</i>							
CFCW	Qwen2.5-7B	0.538	0.452	0.508	0.452	0.588	0.553
	LLaMA3-8B	<u>0.573</u>	<u>0.513</u>	0.548	0.487	0.678	0.583
PBFG	Qwen2.5-7B	0.568	0.487	<u>0.573</u>	<u>0.513</u>	0.683	0.543
	LLaMA3-8B	0.482	0.372	<u>0.673</u>	<u>0.508</u>	0.834	0.623
<i>Domain II: Mathematical Reasoning</i>							
CountProb	Qwen2.5-7B	0.533	0.487	<u>0.558</u>	<u>0.538</u>	0.578	0.573
	LLaMA3-8B	<u>0.427</u>	0.382	0.422	<u>0.397</u>	0.508	0.497
Geometry	Qwen2.5-7B	0.613	0.583	<u>0.628</u>	<u>0.608</u>	0.724	0.709
	LLaMA3-8B	<u>0.457</u>	<u>0.437</u>	0.452	0.432	0.638	0.613
<i>Domain III: Multimodal Understanding</i>							
MC	LLaVA-7B	0.131	0.121	0.090	0.035	0.146	0.141
	Qwen2.5-VL-7B	0.131	0.136	<u>0.146</u>	<u>0.156</u>	0.236	0.231
RG	LLaVA-7B	0.256	0.261	<u>0.357</u>	<u>0.327</u>	0.432	0.417
	Qwen2.5-VL-7B	<u>0.231</u>	<u>0.226</u>	0.151	0.166	0.261	0.256

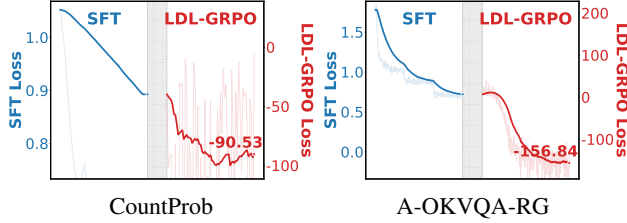


Figure 2. Two-stage convergence behavior from *SFT* to *LDL-GRPO*. The dashed vertical line marks the transition from *SFT* (Stage I) to *LDL-GRPO* (Stage II). Results are shown for CountProb with LLaMA3-8B and A-OKVQA-RG with LLaVA-1.5-7B. Across unimodal and multimodal tasks, *LDL-GRPO* exhibits stable loss trajectories after the transition, without sudden divergence.

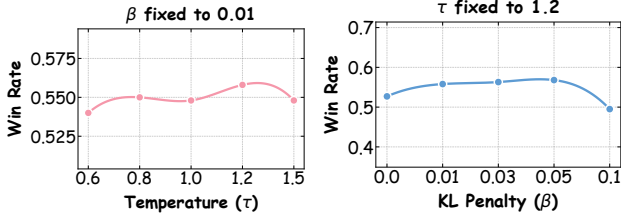


Figure 3. Sensitivity analysis on CountProb (LLaMA3-8B). Representative sweeps with fixed β (left) and fixed τ (right).

that the gains arise from genuine enhancements in response quality rather than increased verbosity.

4.4. Convergence Analysis

Figure 2 illustrates the two-stage training dynamics from *SFT* to *LDL-GRPO*. After switching to *LDL-GRPO*, both unimodal (CountProb) and multimodal (A-OKVQA-RG)

settings exhibit stable loss trajectories without abrupt oscillation or collapse. This indicates that anchor-conditioned and LDL-based group supervision enables a smooth transition from imitation learning to preference optimization, even in challenging multimodal reasoning tasks. We provided additional results of the convergence analysis in Appendix G.

4.5. Hyperparameter Sensitivity Analysis

As shown in Figure 3, our method is insensitive to moderate variations of the sampling temperature τ and the KL penalty β on CountProb with LLaMA3-8B. With $\beta = 0.01$ fixed, sweeping $\tau \in [0.6, 1.5]$ yields a nearly flat win-rate curve, indicating stable performance across a wide sampling regime. With $\tau = 1.2$ fixed, small-to-moderate β values maintain comparable performance, whereas overly large β noticeably degrades win rate, suggesting that excessive KL regularization restricts policy improvement. Based on this analysis, we adopt $\tau = 1.2$ and $\beta = 0.01$ in all experiments. Due to the limited space, more results of hyperparameter sensitivity analysis can be found in Appendix G.

5. Conclusion

In this work, we study a practical challenge that on-premise small expert models often stop at *SFT* and fail to benefit from a second-stage preference-optimization loop due to the high cost of human feedback, reward-model construction, and repeated teacher scoring. To address this, we propose an anchor-guided and fully local alignment strategy that queries a black-box teacher only once per prompt to obtain

an anchor, and then relies on local multi-response sampling and self-evaluation to induce training signals for preference optimization. Building on this setup, we introduce *LDL-GRPO*, which converts anchor-induced comparisons into label-distribution-style group supervision and performs stable group-relative policy optimization. Across unimodal and multimodal benchmarks, the proposed method outperforms SFT-only and anchor-guided RL baselines under raw and length-controlled win rates, making SFT-to-RL practical for strict on-premise deployment.

References

Bai, S., Chen, K., Liu, X., Wang, J., Ge, W., Song, S., Dang, K., Wang, P., Wang, S., Tang, J., et al. Qwen2. 5-vl technical report. *arXiv preprint arXiv:2502.13923*, 2025.

Bai, Y., Kadavath, S., Kundu, S., Askell, A., Kernion, J., Jones, A., Chen, A., Goldie, A., Mirhoseini, A., McKinnon, C., et al. Constitutional ai: Harmlessness from ai feedback. *arXiv preprint arXiv:2212.08073*, 2022.

Boyd, S. and Vandenberghe, L. *Convex optimization*. Cambridge university press, 2004.

Casper, S., Davies, X., Shi, C., Gilbert, T. K., Scheurer, J., Rando, J., Freedman, R., Korbak, T., Lindner, D., Freire, P., et al. Open problems and fundamental limitations of reinforcement learning from human feedback. *arXiv preprint arXiv:2307.15217*, 2023.

Ethayarajh, K., Xu, W., Muennighoff, N., Jurafsky, D., and Kiela, D. Kto: Model alignment as prospect theoretic optimization. *arXiv preprint arXiv:2402.01306*, 2024.

Fan, A., Lewis, M., and Dauphin, Y. Hierarchical neural story generation. *arXiv preprint arXiv:1805.04833*, 2018.

Garg, S., Wu, Y., Smola, A. J., Balakrishnan, S., and Lipton, Z. Mixture proportion estimation and pu learning: A modern approach. In *NeurIPS*, pp. 8532–8544, 2021.

Gou, J., Yu, B., Maybank, S. J., and Tao, D. Knowledge distillation: A survey. *International Journal of Computer Vision*, 129(6):1789–1819, 2021.

Grattafiori, A., Dubey, A., Jauhri, A., Pandey, A., Kadian, A., Al-Dahle, A., Letman, A., Mathur, A., Schelten, A., Vaughan, A., et al. The llama 3 herd of models. *arXiv preprint arXiv:2407.21783*, 2024.

Gunasekar, S., Zhang, Y., Aneja, J., Mendes, C. C. T., Del Giorno, A., Gopi, S., Javaheripi, M., Kauffmann, P., de Rosa, G., Saarikivi, O., et al. Textbooks are all you need. *arXiv preprint arXiv:2306.11644*, 2023.

Guo, D., Yang, D., Zhang, H., Song, J., Zhang, R., Xu, R., Zhu, Q., Ma, S., Wang, P., Bi, X., et al. Deepseek-r1: Incentivizing reasoning capability in llms via reinforcement learning. *arXiv preprint arXiv:2501.12948*, 2025.

He, J., Lin, H., Wang, Q., Fung, Y. R., and Ji, H. Self-correction is more than refinement: A learning framework for visual and language reasoning tasks. In *ACL Findings*, pp. 6405–6421, 2025.

Hendrycks, D., Burns, C., Kadavath, S., Arora, A., Basart, S., Tang, E., Song, D., and Steinhardt, J. Measuring mathematical problem solving with the math dataset. *arXiv preprint arXiv:2103.03874*, 2021.

Hinton, G., Vinyals, O., and Dean, J. Distilling the knowledge in a neural network. *arXiv preprint arXiv:1503.02531*, 2015.

Hsieh, C.-Y., Li, C.-L., Yeh, C.-K., Nakhos, H., Fujii, Y., Ratner, A., Krishna, R., Lee, C.-Y., and Pfister, T. Distilling step-by-step! outperforming larger language models with less training data and smaller model sizes. In *ACL Findings*, pp. 8003–8017, 2023.

Kim, Y. and Rush, A. M. Sequence-level knowledge distillation. In *EMNLP*, pp. 1317–1327, 2016.

Kiryo, R., Niu, G., Du Plessis, M. C., and Sugiyama, M. Positive-unlabeled learning with non-negative risk estimator. In *NeurIPS*, 2017.

Lee, H., Phatale, S., Mansoor, H., Mesnard, T., Ferret, J., Lu, K., Bishop, C., Hall, E., Carbune, V., Rastogi, A., et al. Rlaif vs. rlhf: Scaling reinforcement learning from human feedback with ai feedback. *arXiv preprint arXiv:2309.00267*, 2023.

Li, G., Li, X., Wang, Y., Zhang, S., Wu, Y., and Liang, D. Knowledge distillation for object detection via rank mimicking and prediction-guided feature imitation. In *AAAI*, pp. 1306–1313, 2022.

Li, H., Chen, Y., Luo, J., Wang, J., Peng, H., Kang, Y., Zhang, X., Hu, Q., Chan, C., Xu, Z., et al. Privacy in large language models: Attacks, defenses and future directions. *arXiv preprint arXiv:2310.10383*, 2023a.

Li, L., Zhang, Y., and Chen, L. Prompt distillation for efficient llm-based recommendation. In *CIKM*, pp. 1348–1357, 2023b.

Lin, A., Wohlwend, J., Chen, H., and Lei, T. Autoregressive knowledge distillation through imitation learning. *arXiv preprint arXiv:2009.07253*, 2020.

Liu, A., Feng, B., Xue, B., Wang, B., Wu, B., Lu, C., Zhao, C., Deng, C., Zhang, C., Ruan, C., et al. Deepseek-v3 technical report. *arXiv preprint arXiv:2412.19437*, 2024.

Liu, H., Li, C., Wu, Q., and Lee, Y. J. Visual instruction tuning. In *NeurIPS*, pp. 34892–34916, 2023.

Madaan, A., Tandon, N., Gupta, P., Hallinan, S., Gao, L., Wiegreffe, S., Alon, U., Dziri, N., Prabhumoye, S., Yang, Y., et al. Self-refine: Iterative refinement with self-feedback. In *NeurIPS*, pp. 46534–46594, 2023.

Niu, G., Du Plessis, M. C., Sakai, T., Ma, Y., and Sugiyama, M. Theoretical comparisons of positive-unlabeled learning against positive-negative learning. In *NeurIPS*, 2016.

Ouyang, L., Wu, J., Jiang, X., Almeida, D., Wainwright, C., Mishkin, P., Zhang, C., Agarwal, S., Slama, K., Ray, A., et al. Training language models to follow instructions with human feedback. In *NeurIPS*, pp. 27730–27744, 2022.

Park, W., Kim, D., Lu, Y., and Cho, M. Relational knowledge distillation. In *CVPR*, pp. 3967–3976, 2019a.

Park, W., Kim, D., Lu, Y., and Cho, M. Relational knowledge distillation. In *CVPR*, pp. 3967–3976, 2019b.

Phuong, M. and Lampert, C. Towards understanding knowledge distillation. In *ICML*, pp. 5142–5151. PMLR, 2019.

Rafailov, R., Sharma, A., Mitchell, E., Manning, C. D., Ermon, S., and Finn, C. Direct preference optimization: Your language model is secretly a reward model. In *NeurIPS*, pp. 53728–53741, 2023.

Schulman, J., Wolski, F., Dhariwal, P., Radford, A., and Klimov, O. Proximal policy optimization algorithms. *arXiv preprint arXiv:1707.06347*, 2017.

Schwenk, D., Khandelwal, A., Clark, C., Marino, K., and Mottaghi, R. A-okvqa: A benchmark for visual question answering using world knowledge. In *ECCV*, pp. 146–162, 2022.

Shridhar, K., Sinha, K., Cohen, A., Wang, T., Yu, P., Pasunuru, R., Sachan, M., Weston, J., and Celikyilmaz, A. The art of llm refinement: Ask, refine, and trust. In *ACL*, pp. 5872–5883, 2024.

Shumailov, I., Shumaylov, Z., Zhao, Y., Gal, Y., Papernot, N., and Anderson, R. The curse of recursion: Training on generated data makes models forget. *arXiv preprint arXiv:2305.17493*, 2023.

Sun, W., Chen, Z., Ma, X., Yan, L., Wang, S., Ren, P., Chen, Z., Yin, D., and Ren, Z. Instruction distillation makes large language models efficient zero-shot rankers. *arXiv preprint arXiv:2311.01555*, 2023.

Thawakar, O., Venkatraman, S., Thawkar, R., Shaker, A., Cholakkal, H., Anwer, R. M., Khan, S., and Khan, F. Evolmm: Self-evolving large multimodal models with continuous rewards. *arXiv preprint arXiv:2511.16672*, 2025.

Tian, Y., Peng, B., Song, L., Jin, L., Yu, D., Han, L., Mi, H., and Yu, D. Toward self-improvement of llms via imagination, searching, and criticizing. In *NeurIPS*, pp. 52723–52748, 2024.

Touvron, H., Martin, L., Stone, K., Albert, P., Almahairi, A., Babaei, Y., Bashlykov, N., Batra, S., Bhargava, P., Bhosale, S., et al. Llama 2: Open foundation and fine-tuned chat models. *arXiv preprint arXiv:2307.09288*, 2023.

Tunstall, L., Beeching, E., Lambert, N., Rajani, N., Rasul, K., Belkada, Y., Huang, S., Von Werra, L., Fourrier, C., Habib, N., et al. Zephyr: Direct distillation of lm alignment. *arXiv preprint arXiv:2310.16944*, 2023.

Wang, L. and Yoon, K.-J. Knowledge distillation and student-teacher learning for visual intelligence: A review and new outlooks. *IEEE Transactions on Pattern Analysis and Machine Intelligence*, 44(6):3048–3068, 2021.

Wang, Y., Kordi, Y., Mishra, S., Liu, A., Smith, N. A., Khashabi, D., and Hajishirzi, H. Self-instruct: Aligning language models with self-generated instructions. In *ACL*, pp. 13484–13508, 2023.

Wei, Y., Hu, Z., Shen, L., Wang, Z., Yuan, C., and Tao, D. Open-vocabulary customization from clip via data-free knowledge distillation. In *ICLR*, 2025.

Xiang, Q., Zhang, M., Shang, Y., Wu, J., Yan, Y., and Nie, L. Dkdm: Data-free knowledge distillation for diffusion models with any architecture. In *CVPR*, pp. 2955–2965, 2025.

Yang, A., Li, A., Yang, B., Zhang, B., Hui, B., Zheng, B., Yu, B., Gao, C., Huang, C., Lv, C., et al. Qwen3 technical report. *arXiv preprint arXiv:2505.09388*, 2025a.

Yang, A., Yu, B., Li, C., Liu, D., Huang, F., Huang, H., Jiang, J., Tu, J., Zhang, J., Zhou, J., et al. Qwen2. 5-1m technical report. *arXiv preprint arXiv:2501.15383*, 2025b.

Yang, Z., Zeng, A., Li, Z., Zhang, T., Yuan, C., and Li, Y. From knowledge distillation to self-knowledge distillation: A unified approach with normalized loss and customized soft labels. In *ICCV*, pp. 17185–17194, 2023.

Yin, X., Wang, X., Pan, L., Lin, L., Wan, X., and Wang, W. Y. Gödel agent: A self-referential agent framework for recursively self-improvement. In *ACL*, pp. 27890–27913, 2025.

Yu, K., Yu, C., Zhang, T., Zhao, X., Yang, S., Wang, H.,
Zhang, Q., and Xu, Q. Temporal separation with entropy
regularization for knowledge distillation in spiking neural
networks. In *CVPR*, pp. 8806–8816, 2025.

Yuan, W., Pang, R. Y., Cho, K., Li, X., Sukhbaatar, S., Xu,
J., and Weston, J. E. Self-rewarding language models. In
ICML, 2024a.

Yuan, W., Pang, R. Y., Cho, K., Li, X., Sukhbaatar, S., Xu,
J., and Weston, J. E. Self-rewarding language models. In
ICML, 2024b.

Zelikman, E., Wu, Y., Mu, J., and Goodman, N. Star:
Bootstrapping reasoning with reasoning. In *NeurIPS*, pp.
15476–15488, 2022.

Zhang, L., Song, J., Gao, A., Chen, J., Bao, C., and Ma,
K. Be your own teacher: Improve the performance of
convolutional neural networks via self distillation. In
ICCV, pp. 3713–3722, 2019.

Zheng, L., Chiang, W.-L., Sheng, Y., Zhuang, S., Wu, Z.,
Zhuang, Y., Lin, Z., Li, Z., Li, D., Xing, E., et al. Judg-
ing llm-as-a-judge with mt-bench and chatbot arena. In
NeurIPS, pp. 46595–46623, 2023.

Zhou, C., Liu, P., Xu, P., Iyer, S., Sun, J., Mao, Y., Ma, X.,
Efrat, A., Yu, P., Yu, L., et al. Lima: Less is more for
alignment. In *NeurIPS*, 2023.

Zhou, Y., Fan, Z., Cheng, D., Yang, S., Chen, Z., Cui, C.,
Wang, X., Li, Y., Zhang, L., and Yao, H. Calibrated
self-rewarding vision language models. In *NeurIPS*, pp.
51503–51531, 2024.

Appendix Table of Contents

A.	Notation and Definition	13
B.	Theoretical Proofs	14
B.1	Proof of Theorem 3.1 (Order Consistency)	14
B.2	Proof of Theorem 3.3 (Near-Optimality)	14
C.	Supplementary Experimental Instructions	16
C.1	Evaluation Protocol and Judge Models	16
C.2	Teacher Query Budget and Cost Analysis	16
C.3	Datasets and Evaluation Tasks	16
C.4	Backbone Models and Implementation Details	17
D.	Limitation	18
E.	Reproducibility	19
F.	Use of LLMs in Writing	19
G.	Supplementary Results	19

A. Notation and Definition

Table A.3. Mathematical notations and definitions

Symbol	Definition
x	A prompt or query (scalar or structured input, e.g., text or multimodal input).
y	A response sequence generated for prompt x .
\mathcal{D}_x	Unlabeled on-premise prompt pool.
T	Black-box teacher model, accessed only via generation.
$a = T(x)$	Teacher-generated response for prompt x , used as an anchor.
$p_{\text{base}}(\cdot x)$	Base student policy before supervised fine-tuning.
$p_{\text{sft}}(\cdot x)$	Student policy after supervised fine-tuning (Stage I).
$p_{\theta}(\cdot x)$	Trainable student policy in Stage II, parameterized by θ .
$p_{\text{ref}}(\cdot x)$	Frozen reference policy for KL regularization (set to p_{sft}).
$U(x) = \{y_k\}_{k=1}^K$	Candidate response set sampled from the student for prompt x .
K	Number of sampled candidate responses per prompt.
$g_{\theta}(x, a, y)$	Anchor-conditioned self-evaluation score produced by the student.
$s^* = g_{\theta}(x, a, a)$	Anchor self-score used as a calibration baseline.
r_k	Anchor-referenced margin for candidate y_k , defined as $r_k = s_k - s^*$.
$\sigma(\cdot)$	Sigmoid function used for PU confidence calibration.
γ	Sharpness parameter controlling PU confidence transition.
τ	Temperature parameter controlling the concentration of softmax weighting.
$D_x \in \Delta^{K-1}$	PU-induced soft preference label distribution over $U(x)$.
$q_{\theta}(y_k x)$	Candidate-normalized student policy probability over $U(x)$.
β	Weight of KL regularization against the reference policy.

B. Theoretical Proofs

B.1. Proof of Theorem 3.1

Proof. Define the function

$$f(r) := \log \sigma(\gamma r) + \frac{r}{\tau}.$$

Then the induced distribution can be written as

$$D_x(k) \propto \exp(f(r_k)).$$

We first show that f is strictly increasing. Taking the derivative,

$$f'(r) = \frac{d}{dr} \log \sigma(\gamma r) + \frac{1}{\tau} = \gamma(1 - \sigma(\gamma r)) + \frac{1}{\tau}.$$

Since $\gamma > 0$, $\tau > 0$, and $0 < \sigma(\gamma r) < 1$, we have

$$f'(r) > 0 \quad \text{for all } r \in \mathbb{R}.$$

Hence f is strictly increasing.

Therefore, for any i, j ,

$$r_i > r_j \implies f(r_i) > f(r_j) \implies \exp(f(r_i)) > \exp(f(r_j)) \implies D_x(i) > D_x(j).$$

This proves that D_x strictly preserves the ordering induced by the margins $\{r_k\}$. \square

B.2. Proof of Theorem 3.2

Proof. We first define the standard softmax distribution

$$\bar{D}(k) := \frac{\exp(r_k/\tau)}{\sum_{j=1}^K \exp(r_j/\tau)},$$

and define the normalization constant

$$Z := \sum_{j=1}^K \exp(r_j/\tau).$$

We then relate $\log Z$ to the expected margin and the entropy of \bar{D} . By definition,

$$\log \bar{D}(k) = \frac{r_k}{\tau} - \log Z.$$

Therefore, the Shannon entropy of \bar{D} satisfies

$$\begin{aligned} H(\bar{D}) &:= - \sum_{k=1}^K \bar{D}(k) \log \bar{D}(k) \\ &= - \sum_{k=1}^K \bar{D}(k) \left(\frac{r_k}{\tau} - \log Z \right) \\ &= - \frac{1}{\tau} \sum_{k=1}^K \bar{D}(k) r_k + \log Z \sum_{k=1}^K \bar{D}(k). \end{aligned}$$

Since $\sum_{k=1}^K \bar{D}(k) = 1$, we obtain

$$\log Z = \frac{1}{\tau} \mathbb{E}_{\bar{D}}[r_k] + H(\bar{D}),$$

which gives

$$\log \sum_{k=1}^K \exp(r_k/\tau) = \frac{1}{\tau} \mathbb{E}_{\bar{D}}[r_k] + H(\bar{D}).$$

Next, we bound the two terms. On the one hand, the entropy is upper-bounded by

$$H(\bar{D}) \leq \log K.$$

On the other hand,

$$\log \sum_{k=1}^K \exp(r_k/\tau) \geq \log \exp(r_{\max}/\tau) = \frac{r_{\max}}{\tau}.$$

Combining the above inequalities yields

$$\mathbb{E}_{\bar{D}}[r_k] \geq r_{\max} - \tau \log K.$$

Observe that D_x can be written as

$$D_x(k) = \frac{\bar{D}(k) \sigma(\gamma r_k)}{\sum_{j=1}^K \bar{D}(j) \sigma(\gamma r_j)}.$$

Since $\sigma(\gamma r)$ is a strictly increasing function of r , multiplying \bar{D} by $\sigma(\gamma r_k)$ shifts probability mass toward larger margins.

Formally, for the random variable R taking values $\{r_k\}$ under \bar{D} , the covariance $\text{Cov}_{\bar{D}}(R, \sigma(\gamma R)) \geq 0$. Thus,

$$\mathbb{E}_{k \sim D_x}[r_k] \geq \mathbb{E}_{k \sim \bar{D}}[r_k].$$

Combining the two steps yields

$$r_{\max} - \mathbb{E}_{k \sim D_x}[r_k] \leq r_{\max} - \mathbb{E}_{k \sim \bar{D}}[r_k] \leq \tau \log K.$$

This completes the proof. \square

C. Supplementary Experimental Instructions

C.1. Evaluation Protocol and Judge Models

Judge Models. For automatic preference evaluation, we use large instruction-tuned foundation models as external judges. Specifically, for unimodal text-only tasks, we adopt Qwen3-235B-A22B-Instruct, available at <https://huggingface.co/Qwen/Qwen3-235B-A22B-Instruct-2507>. For multimodal tasks, we use Qwen3-VL-235B-A22B-Instruct, available at <https://huggingface.co/Qwen/Qwen3-VL-235B-A22B-Instruct>. The judge prompt used for automatic evaluation is shown below.

```
You will judge two responses to the same question.
Choose the better one overall (correctness, grounding, clarity, completeness).
You are given the reference (ground-truth answer) to help judge correctness.
Reply with exactly one character:
A = Response A is better
B = Response B is better
T = Tie / too close to call

==== Question / Prompt ====
{task_prompt}

==== Reference (Ground Truth) ====
{gt}

==== Response A ====
{ans_model}

==== Response B ====
{ans_gpt}
```

Figure C.4. Prompt used for automatic pairwise preference evaluation.

C.2. Teacher Query Budget and Cost Analysis

We summarize the teacher-query complexity of different alignment strategies under a unified setting with N prompts and K candidates per prompt.

Table C.4. Teacher-query complexity comparison.

Method	Teacher Calls Order
<i>SFT</i>	N
<i>SinglePair-DPO</i>	N
<i>Teacher-as-Judge RL</i>	NK
<i>AnchorRank-DPO</i>	N
<i>LDL-GRPO</i>	N

Both *AnchorRank-DPO* and *LDL-GRPO* require only one black-box teacher generation per prompt, while all candidate scoring and policy updates are performed fully on-premise.

C.3. Datasets and Evaluation Tasks

WritingPrompts. We use the WritingPrompts dataset (Fan et al., 2018) for creative writing evaluation. The original dataset is available at <https://arxiv.org/abs/1805.04833>. We construct two variants: (i) WritingPrompts-CW, focusing on constraint-following creative writing, and (ii) WritingPrompts-EU, emphasizing expressive and stylistic diversity. Table C.5 provides representative examples from the WritingPrompts dataset used in our evaluation, including the input prompt and model-generated responses.

Table C.5. Representative examples from the WritingPrompts dataset.

Field	Content
Prompt (Case 1)	<i>[EU]</i> As a treat to fans, George R. R. Martin writes a character inspired by himself into the final book of the <i>A Song of Ice and Fire</i> series. That character suffers the most gruesome fate of all.
Reference	A dramatic courtroom-style scene in which the author-character is judged and sentenced, written with dark humor and theatrical dialogue.
Model Output	A narrative depicting the author-character pleading innocence before being condemned to a brutal fate, featuring exaggerated dialogue, irony, and grim imagery consistent with the prompt.
Prompt (Case 2)	<i>[CW]</i> Each character can only speak one sentence.
Reference	A tense short story set aboard a damaged submarine, where each character’s single-sentence dialogue advances the plot toward a sacrificial ending.
Model Output	A compact narrative obeying the one-sentence-per-character constraint, using internal monologue and sparse dialogue to convey urgency and moral tension.

Table C.6. Representative examples from the Competition Math dataset used in our evaluation.

Subset	Prompt	Ground Truth Answer
CompMath-Count	Solve the following competition math problem: Bob’s password consists of a non-negative single-digit number followed by a letter and another non-negative single-digit number (which could be the same as the first one). What is the probability that Bob’s password consists of an odd single-digit number, followed by a letter, and a positive single-digit number?	Exactly 5 out of the 10 non-negative single-digit numbers are odd, giving probability $\frac{1}{2}$. The second character is always a letter. For the last character, 9 out of 10 digits are positive. Thus, the desired probability is $\frac{1}{2} \times 1 \times \frac{9}{10} = \boxed{\frac{9}{20}}$.
CompMath-Geometry	Solve the following competition math problem: A wire is cut into two pieces, one of length a and the other of length b . The piece of length a is bent to form an equilateral triangle, and the piece of length b is bent to form a regular hexagon. If the triangle and the hexagon have equal area, what is $\frac{a}{b}$?	The triangle side length is $\frac{a}{3}$ and its area is $\frac{\sqrt{3}}{4} \left(\frac{a}{3}\right)^2 = \frac{a^2 \sqrt{3}}{36}$. The hexagon side length is $\frac{b}{6}$ and its area is $\frac{3\sqrt{3}}{2} \left(\frac{b}{6}\right)^2 = \frac{b^2 \sqrt{3}}{24}$. Equating the two areas yields $\frac{a^2}{b^2} = \frac{3}{2}$, hence $\frac{a}{b} = \boxed{\frac{\sqrt{6}}{2}}$.

Competition Math. We evaluate mathematical reasoning using the Competition Math dataset (Hendrycks et al., 2021), available at <https://arxiv.org/abs/2103.03874>. We report results on two subsets: CompMath-Count, which emphasizes counting and arithmetic reasoning, and CompMath-Geometry, which focuses on geometric problem solving. Table C.6 provides representative examples from the Competition Math dataset used in our evaluation, including the input prompt and model-generated responses.

A-OKVQA. For multimodal evaluation, we use the A-OKVQA benchmark (Schwenk et al., 2022), available at <https://arxiv.org/abs/2206.01718>. We consider two tasks: A-OKVQA-MC, a multiple-choice VQA task, and A-OKVQA-Rationale, which requires generating free-form rationales grounded in the image content. Table C.7 provides representative examples from the A-OKVQA dataset used in our evaluation, including the input prompt and model-generated responses.

C.4. Backbone Models and Implementation Details

For unimodal on-premise deployment, we use Qwen2.5-7B-Instruct (<https://huggingface.co/Qwen/Qwen2.5-7B-Instruct>) and LLaMA3-8B-Instruct (<https://huggingface.co/meta-llama/Meta-Llama-3-8B-Instruct>).

Table C.7. Example cases from the A-OKVQA benchmark used in our evaluation.

Task	Prompt (Image + Question)	Ground Truth Output
A-OKVQA-MC	Question: What color is reflected strongly off the metal cabinet cases? Options: (0) purple (1) red (2) blue (3) yellow	Answer: red
A-OKVQA-Rationale	Question: What does he use to build momentum? (The input includes an image of a person skateboarding.)	Rationale: A guy is on a skateboard as he cruises down the street. He uses the bottom part of his leg to push against the ground and propel himself forward.

For multimodal tasks, we use LLaVA-7B (<https://github.com/haotian-liu/LLaVA>) and Qwen2.5-VL-7B-Instruct (<https://huggingface.co/Qwen/Qwen2.5-VL-7B-Instruct>).

All models are deployed locally without external API calls during alignment and evaluation.

Anchor-conditioned self-evaluation (scalar scoring). For each query x , an anchor response a generated by the teacher, and a candidate response y sampled from the student, we prompt the student to perform anchor-conditioned self-evaluation as follows:

Question:

A jar contains 7 red marbles and 5 blue marbles. Two marbles are drawn without replacement. What is the probability that both marbles are red?

Reference Answer:

There are $\binom{12}{2}$ ways to draw 2 marbles. Favorable outcomes are drawing 2 from the 7 red marbles: $\binom{7}{2}$. Thus the probability is $\frac{\binom{7}{2}}{\binom{12}{2}} = \frac{21}{66} = \frac{7}{22}$.

Candidate Answer:

The probability is $(7/12) \cdot (6/11) = 42/132 = 7/22$.

Scalar Score (example output): 0.95

Anchor self-calibration. To calibrate scores under the positive–unlabeled setting, we also evaluate the anchor against itself using the same prompt structure. Specifically, we set the candidate answer to be identical to the anchor:

Question:

A fair coin is flipped 4 times. What is the probability of getting exactly 3 heads?

Reference Answer:

There are $\binom{4}{3} = 4$ sequences with exactly 3 heads, and $2^4 = 16$ total outcomes, so the probability is $4/16 = 1/4$.

Candidate Answer:

There are $\binom{4}{3} = 4$ sequences with exactly 3 heads, and $2^4 = 16$ total outcomes, so the probability is $4/16 = 1/4$.

Scalar Score (example output): 1.00

D. Limitation

While our method enables a fully local and low-cost alignment pipeline under strict on-premise constraints, it still relies on several design choices that need further investigation. First, the quality of the induced preference signal depends on the

student’s anchor-conditioned self-evaluation, which may be imperfect when the student is still relatively weak or when the task requires fine-grained judgment. Although the proposed PU formulation and label-distribution learning help mitigate noise and instability, exploring more robust self-evaluation mechanisms remains an interesting direction. Second, our current implementation requires sampling multiple candidates per prompt to construct group-level supervision, which introduces additional computation compared to single-response updates. Improving the efficiency of candidate generation and reuse, or reducing the required group size without hurting stability, is left for future work.

E. Reproducibility

We provide implementation details, involving illustrative algorithm descriptions in Section 3, Section 4, and Appendix C, and pseudo-code in Algorithm 1. The code will be publicly released for reproducibility.

F. Use of LLMs in Writing

We used a large language model (LLM) solely to polish the writing and correct grammatical issues during the preparation of this paper. The LLM was not involved in idea generation, experiment design, or analysis. All scientific contributions are entirely made by the authors.

G. Supplementary Results

Two-stage convergence from SFT to LDL-GRPO. Figures C.5 and C.6 visualize the training dynamics of our two-stage pipeline on representative model–task pairs. In each panel, the *SFT stage* (blue; left y-axis) exhibits a smooth decrease of the supervised objective, indicating stable imitation learning. After switching to *LDL-GRPO* (red; right y-axis; gray band marks the transition), the *LDL-GRPO* objective consistently drops and then stabilizes, demonstrating that anchor-induced group supervision yields a well-behaved preference-optimization signal. Importantly, we observe no abrupt divergence or oscillation across both unimodal writing tasks (*e.g.*, CountProb, Geometry, CFCW, PBFG) and multimodal benchmarks (*e.g.*, MC, RG), and the same stable trend holds for different backbones (*e.g.*, LLaMA3-8B, Qwen2.5-7B, LLaVA/Qwen2.5-VL).

Compact sensitivity plots. Figures C.7 and C.8 provide compact sweeps over the sampling temperature τ and KL penalty β on CountProb and A-OKVQA-RG, respectively. Across fixed- β sweeps, the win rate remains largely flat over a wide range of τ , suggesting that our anchor-guided training is not overly sensitive to sampling stochasticity. Across fixed- τ sweeps, small to moderate β values achieve comparable performance, whereas overly large β tends to reduce win rate, consistent with over-regularization that restricts policy improvement. These results support that LDL-GRPO has a broadly stable operating region for hyperparameters.

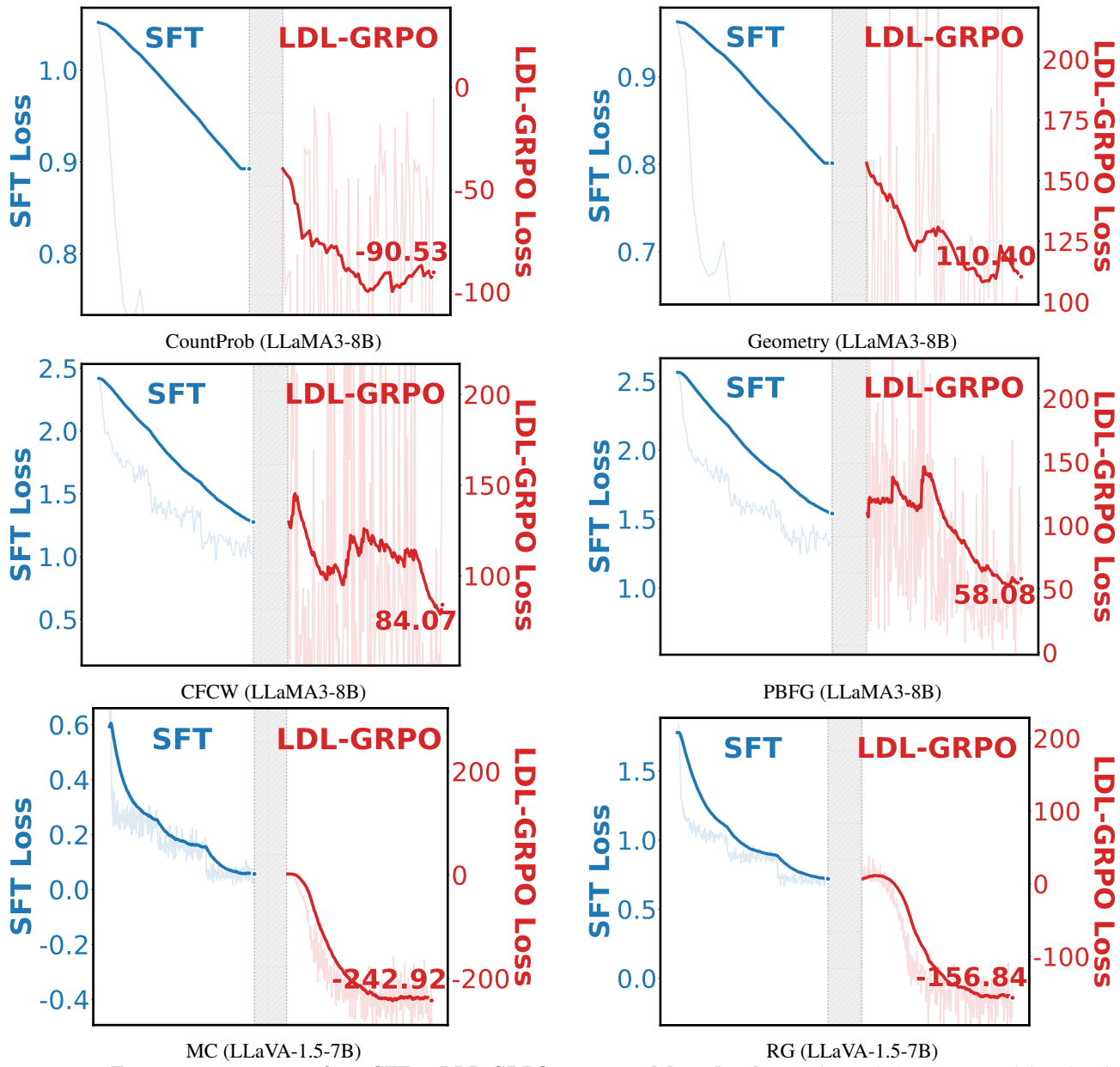


Figure C.5. Two-stage convergence from SFT to LDL-GRPO across models and tasks. Each panel shows one model–task pair, illustrating a stable transition from SFT to LDL-GRPO.

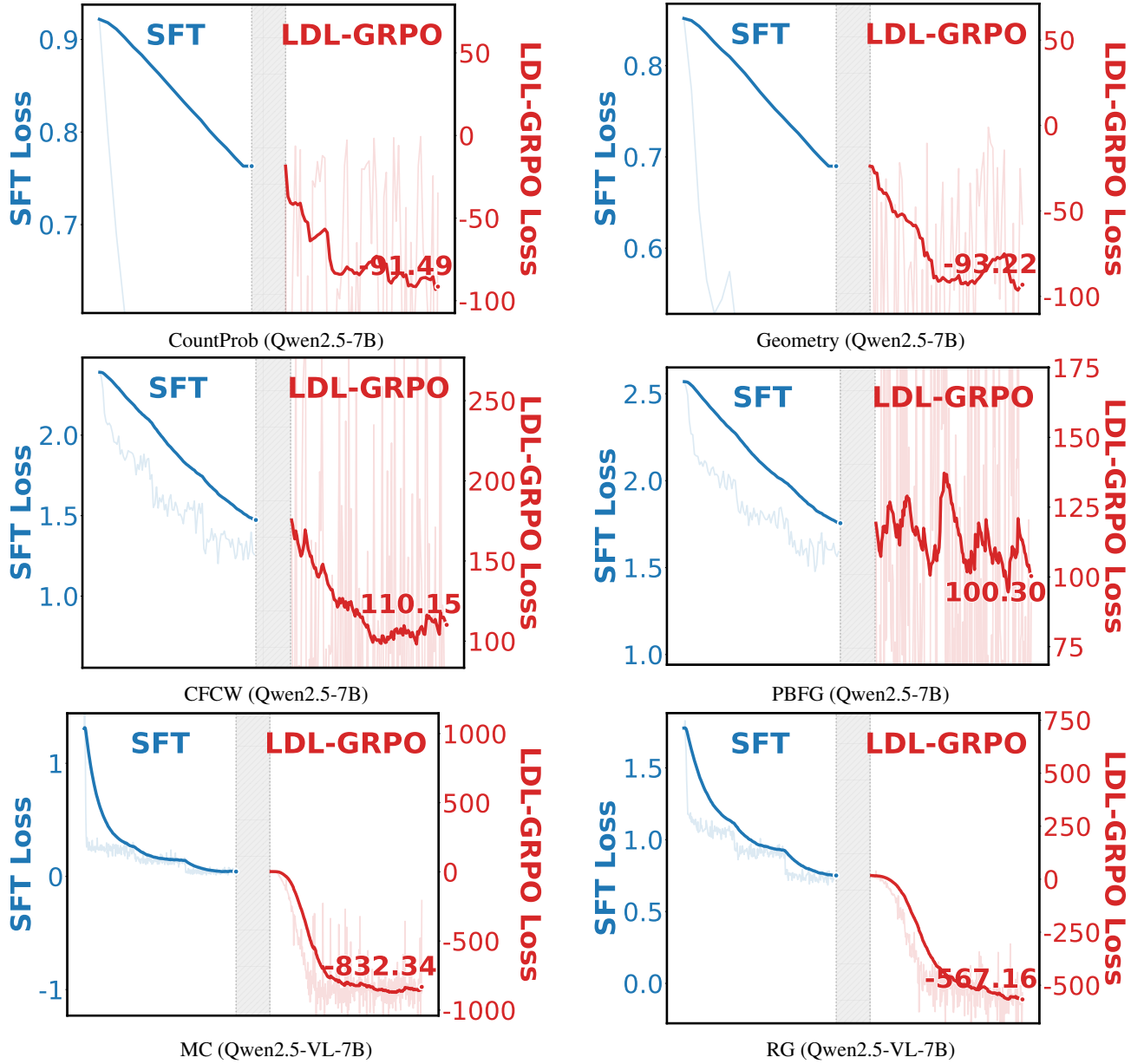


Figure C.6. **Two-stage convergence from SFT to LDL-GRPO across models and tasks.** Each panel shows one model–task pair, illustrating a stable transition from SFT to LDL-GRPO.

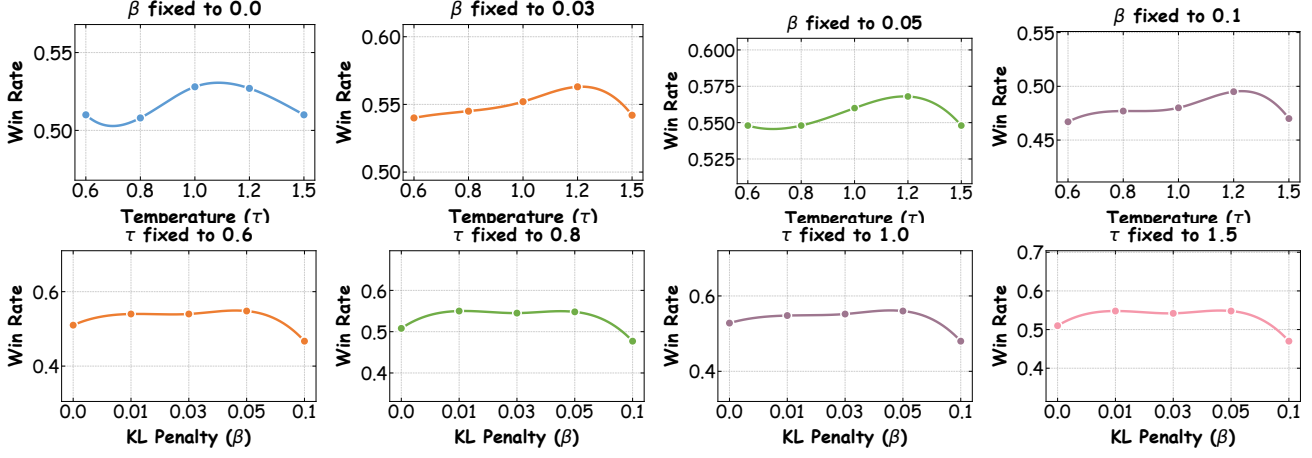


Figure C.7. Compact sensitivity plots on CountProb (LLaMA3-8B). Top: fixed- β sweeps; bottom: fixed- τ sweeps.

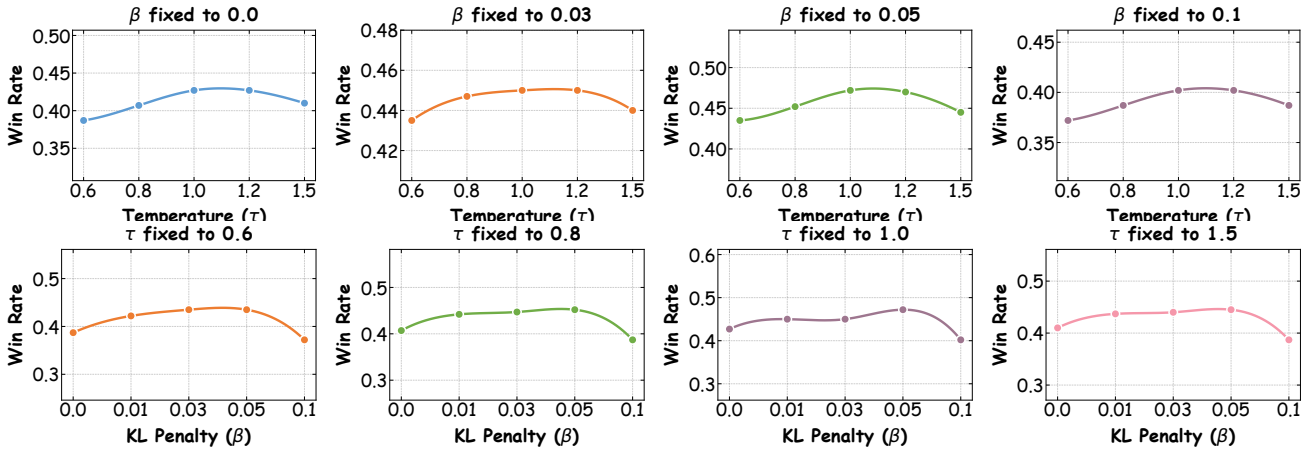


Figure C.8. Compact sensitivity plots on A-OKVQA-RG (LLaVA-7B). Top: fixed- β sweeps; bottom: fixed- τ sweeps.